Laboratory Investigation of Compacted Clay-Sand Soils Used for River Dyke Construction

Anand Panta
Department of Civil Engineering
Lumbini Engineering,
Management and Science College
(Affiliated to Pokhara University)
Rupandehi, Nepal
anandpanta123@gmail.com

Satoshi Nishimura
Faculty of Engineering
Hokkaido University
Sapporo, Japan
nishimura@eng.hokudai.ac.jp

***Abstract*— For the design and stability analysis of embankments, strength and stiffness properties of compacted clay-sand mixed soils with varying water content and dry unit weight are necessary. A widely applicable linear Mohr-Coulomb strength criterion can be used for the interpretation of the strength of such soils, but the strength parameters, particularly apparent cohesion as a result of dilation in densely compacted specimens produced an uncertainty in the calculation of factor of safety for the shallow slope stability analysis. In this study, a series of constant-volume direct shear tests and unconfined compression tests were performed on the compacted specimens of two different clay-sand mixed soils to investigate the undrained strength behaviour. The undrained effective and total stresses strength parameters were derived, which indicated that the apparent cohesion was significant for the state close to the optimum but decreased gradually towards the wetter side, but the angle of internal friction did not show significant variation between the states. Finally, the unconfined compressive strength and deformation modulus increased with decreasing water content, increasing dry unit weight and increasing degree of compaction (the ratio of in-situ dry density to maximum dry density from the laboratory compaction tests) following power functions.**

Keywords*— *Compacted Soil, Compaction States, Undrained Strength, Apparent Cohesion, Dilation

I. INTRODUCTION

Most of the embankments, such as highway or railway embankments, river dykes etc., are found to be made up of compacted fine-grained soils which generally composed of mixtures of clay, silt and sand. The properties (strength, stiffness, and permeability) of such compacted soils are strongly dependent on the compaction state which is generally defined in term of water content and dry unit weight [1-3]. For the design and stability analysis of the embankments, it is therefore necessary to understand clearly the strength and stiffness properties of such compacted mixed soils in relation with different compaction states, particularly water contents and densities as variables, before placing the mixture in its final site. Common practice is to construct the embankments by compacting soils above a specified minimum dry density and a range of water content on the basis of standard proctor compaction carried out in laboratory [4]. The range of water content is usually set at or closer to the optimum either on a wet or a dry side.

Microstructure of compacted specimens is dependent on the molding water content relative to the optimum water content, and the important features governing the compacted soil behavior are the flocculated microstructure on the dry side and the dispersed microstructure on the wet side [5-6]. The fabric of these compacted specimens on the dry side of the optimum composed of aggregates of various sizes with bimodal pore size distribution and discontinuous water phase, while on the wet side of the optimum the fabric is dominated by a more homogenous matrix with a single pore size distribution and continuous water phase [7]. Santucci de Magistris and Tatsuoka [8] conducted a study by performing triaxial compression tests on the compacted specimens of silty-sand and reported that the soil compacted with different water contents produced materials with different microstructures, which affected significantly the stress-strain behavior, and the difference was noticeable at small strains. The strength and stiffness of as-compacted soil usually increases with decreasing water content, increasing dry density and increasing confining pressures. However, it is also evidenced that the soil compacted at low water content collapses upon wetting and the strength can be smaller than those prepared at the optimum.

Interpretation of shear strength of compacted soils can be done by using a linear Mohr-Coulomb strength criterion, $\tau=c'+\sigma'\tan\Phi'$, where, c'=cohesion and Φ'=friction. The cohesion intercept (c') always produces an uncertainty while using the strength parameters in the shallow slope stability analysis [9]. In the compacted specimens, it is usually not possible to have a true cohesion. Hence the cohesion intercept from shear tests in the compacted specimens is an apparent cohesion resulting from the capillary action and interlocking due to dilation. The capillary action and the degree of dilation in the compacted specimens are functions of molding water content and dry unit weight. Field observation showed that most of the slopes began to fail along a potential failure surface when the soil was getting wet and saturated e.g. rainfall-induced instability. Thus more relevant

testing condition for such failure mechanism in a direct shear apparatus could be shearing under a fully submerged condition which reduced the effect of capillary action; and then the apparent cohesion is only due to the dilation, which is usually less well characterized in the factor of safety analysis in practice.

The present study aims to increase understanding of how the compaction state and resulting microstructure influence the strength and stiffness behavior of compacted clay-sand mixed soils sampled from two different river dyke construction sites of Ebesubuto and Higashinosato. The experimental study includes a series of constant-volume direct shear tests under fully submerged condition at low to medium consolidation stress ranges (5-400kPa) and unconfined compression tests on the compacted samples adopting water contents (1.05-1.30w_{opt}) on the wet of optimum. The undrained effective stress paths and strength envelopes for different states by adopting the linear Mohr-Coulomb strength criterion were analyzed and which gave insights into variations of strength parameters as a result of differences in densities and degrees of dilatation during shearing. In addition, the effects of compaction state on unconfined compressive strength and deformation modulus (E_{50}) were also evaluated.

II. EXPERIMENTAL DETAILS

A. Tested Materials

In this study, two clay-sand mixed soil samples were tested, which were sampled from river dyke construction sites in Ebetsubuto and Higashinosato, Hokkaido, Japan. Both samples were on-site mixtures of locally available alluvial clay and volcanic sand in the proportion of approximately 1:1 by weight, and collected after the construction of river dikes. The physical properties are listed in **Table 1**. The particle size distribution curves are presented in **Fig. 1**. The curves show both soils are of highly non-uniform gradations with particle sizes ranging from finer clay to coarser gravel. The standard proctor compaction curves are presented in **Fig. 2**, which show the maximum dry density, optimum water content and the states adopted for the preparation of compacted samples in laboratory.

The compacted samples were prepared by compacting soils in a standard proctor mold with the compaction energy same as the standard proctor test (i.e. 598kJ/m^3) in three different layers, adopting three different water contents of 1.05w_{opt}, 1.15w_{opt}, and 1.30w_{opt}. Each layer received 25 numbers of blows and gave a direct shear test specimen with less inter-variability in compaction between different specimens. These samples were in well-compacted states with degrees of compaction, which is defined as the ratio of dry unit weight of compacted samples to maximum dry unit weight from the standard proctor compaction curve, lying between 88 and 98%, which were relevant to the actual embankment compaction in the sites in Hokkaido. The further details of material properties and specimen preparation methods are presented by Panta [10]. The direct shear test specimen of size 60mm in diameter and 30mm high, the constant-rate-of-strain (CRS) oedometer test specimen of size 60mm in diameter and 20mm high and the unconfined compression test specimen of size 50mm in diameter and 100mm high were trimmed from the large standard proctor test specimens of size 100mm in diameter and 125mm high.

Table 1. Physical properties of tested soils

Name of soils	w_n[(1)] [%]	w_p [%]	w_l[(2)] [%]	G_s	Clay fraction[(3)] [%]	Sand/ Gravel [%]
Ebetsubuto	31.7	29	59	2.64	36/40	35/17
Higashinosato	31.8	25	54	2.58	36/44	50/60

(1) As measured in field after compaction
(2) Measured for constituents passing through a 425μm sieve
(3) (Finer than 2μm)/(Finer than 5μm)

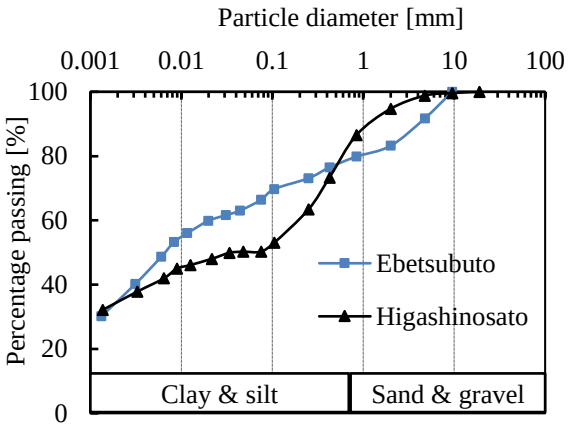

Fig. 1. Particle size distribution curves for tested soils

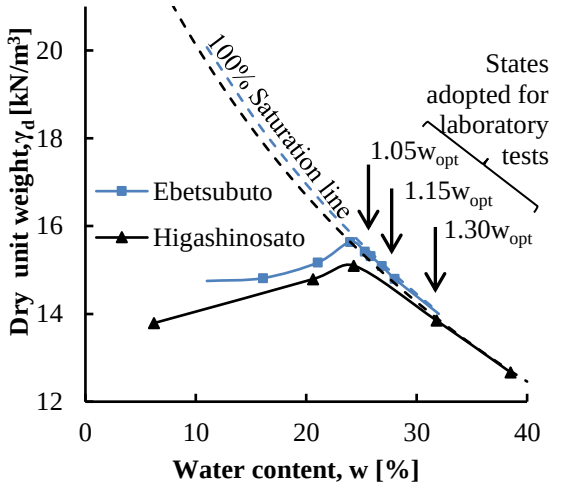

Fig. 2. Standard proctor compaction curves for tested soils

III. METHODS OF TESTING

In this study, the undrained shear strength of soil was tested by conducting a series of constant-volume direct shear tests, which is equivalent to consolidated-undrained triaxial tests, on the compacted samples of Ebetsubuto and Higashinosato

soils. The tests were performed in a fully submerged condition at low to medium consolidation stress ranges of 5-400kPa. The specimens were firstly allowed to swell or consolidate fully to a desired consolidation stress (1.e. 5, 10, 20, 50 and 400 kPa in a series) and then shear under a constant volume and a fully submerged condition at a horizontal displacement rate of 0.01mm/min. This strain rate was found by experience sufficiently slow to equalize the pore water pressure throughout the specimen during shearing to obtain a representative undrained effective stress path. The details of direct shear apparatus and test procedure employed in this study were also reported by Panta and Nishimura [11]. In addition, the unconfined compressive strength of each state was also determined by performing a series of unconfined compression tests with a strain rate of 0.75mm/min.

IV. Results and Discussions

A. *Undrained effective stress paths and strength envelopes*

The undrained effective stress paths and effective strength envelopes for different states of Ebetsubuto and Higashinosato soils obtained from the constant-volume direct shear tests, which are plotted for horizontal shear stress against vertical effective stress, are presented in **Figs. 3(a)** and **(b)**. The stress path for each state showed initially modestly contractive behavior followed by strongly dilative behavior with a distinct peak state at a low consolidation stress range (σ_{v0}'= 5-50kPa), whereas at a high consolidation stress range (σ_{v0}'= 400kPa) the stress paths showed contractive behavior until reaching a failure state and then it moved along the failure envelope indicating the influence of coarser sand and gravel particles. Similar behavior was also observed by Santucci De Magistris and Tatsuoka [8] on compacted silty-sand specimens by performing triaxial compression tests. They reported that the dilatancy characteristics in the compacted specimens are mainly due to the instantaneous dry density which is controlled by the molding water content. The specimens compacted closer to the optimum water content exhibited the strongest tendency of dilation than the wetter specimens. A test series on Higashinosato soil for the state of $1.05w_{opt}$ was not complete due to time limitation during this study. The effective stress strength envelopes are drawn by taking points on the stress paths corresponding to maximum stress ratio (τ/σ_v') using the linear Mohr-Coulomb failure criterion. **Figs. 4 (a)** and **(b)** show the horizontal shear stress versus horizontal displacement curves obtained from the constant-volume direct shear tests with different consolidation stresses. The compacted specimens at the low consolidation stress range (σ_{v0}'= 5-50kPa) showed distinct peak states at low strains followed by strain softening, while at the higher stress range (σ_{v0}'= 400kPa), the peak state was not clearly visible and the dilation was still continue until reaching a maximum displacement of 6mm. The effect of dry density or molding water content on the shear stress at a constant strain was found to be significant, and was more noticeable between the specimens closer to the optimum relative to the wetter specimens because of the effect of dilatancy characteristics on the shear stress. They showed significantly different stress-strain behavior even at higher strains.

The strength envelopes are fitted well with the linear Mohr-Coulomb failure criterion (R^2>0.99), as shown in **Figs. 3(a)** and **(b)**. The Mohr-Coulomb strength parameters are derived and presented in **Table 2**. Due to the strongly dilative behavior of effective stress paths at the low stress range, it may have produced non-linearity in the strength envelopes and affected the interpretation of strength parameters, particularly the apparent cohesion, which could play an important role in the calculation of factor of safety for the shallow slope stability analysis based on the effective stress approach, as mentioned earlier. The past study considering the non-linearity of strength envelopes by using a non-linear power-law strength criterion on clays and similar clay-sand mixed Maizuru soil was carried out and presented by Panta and Nishimura [11]. The results on the clay-sand mixed Maizuru soil showed degrees of non-linearity of power-law effective strength envelopes were in a range of 0.93-0.95, which were close to unity. It means that the failure envelope was approximately linear. Therefore, the linear Mohr-Coulomb failure criterion may be applicable in this study. It can be seen from the table that the values of apparent cohesion for Ebetsubuto soil was significantly high for the states of $1.05w_{opt}$, and $1.15w_{opt}$ (11.2kPa and 8.9kPa, respectively), whereas it was less significant (3.9kPa) for the state of $1.30w_{opt}$. These differences in the apparent cohesion (c') can be explained by the increasing dry density or degree of compaction (about 10%) and resulting degree of dilation during shearing between these states. On the other hand, the friction angle did not show significant variations between these states in comparison to the apparent cohesion. The result is also consistent with the one that observed with the different states of Higashinosato soil. Therefore, with these observations, it can be highlighted that the cohesion values are more sensitive to molding characteristics than the friction angles.

For the short-term stability analysis using conventional limit equilibrium methods, the undrained strength envelopes in terms of total stress is required as the analysis does not involve excess pore water pressure prediction. The total strength envelopes for different states of Ebetsubuto and Higashinoto soils are presented in **Fig. 5**, which are fitted well with the linear Mohr-Coulomb failure criterion (R^2>0.99). The strength parameters are listed in **Table 3**. The cohesion intercept was significantly

high closer to the optimum and which decreased gradually away from the optimum on the wetter side (25.3-11.6kPa for Ebetsubuto soil and 23.1-12.8kPa for Higashinosato soil); this characteristic is similar to that of the effective stress strength envelopes, as mentioned earlier, whereas, the friction angle did not show significant variations between different states as that of the cohesion intercept.

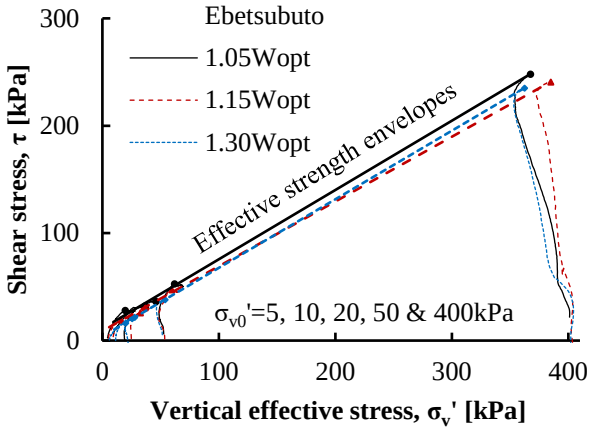

(a)

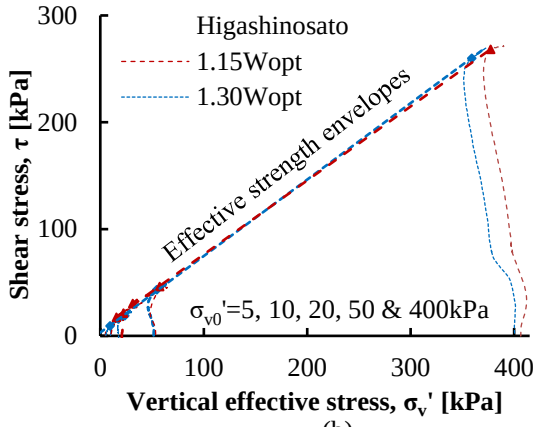

(b)

Fig. 3. Undrained effective stress paths and effective strength envelopes for different states of (a) Ebetsubuto soil (b) Higashinsato soil

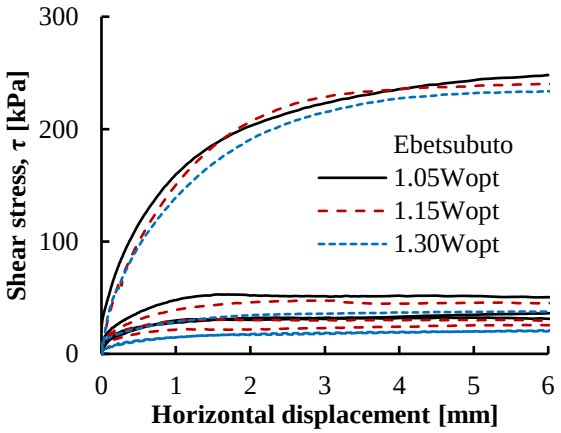

(a)

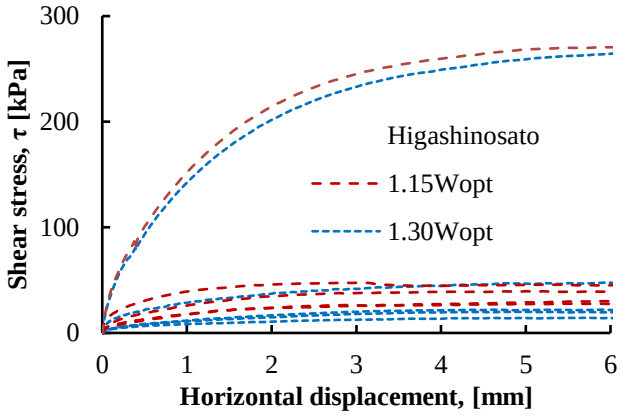

(b)

Fig. 4. Stress-strain curves for different states of (a) Ebetsubuto soil (b) Higasinosato soil

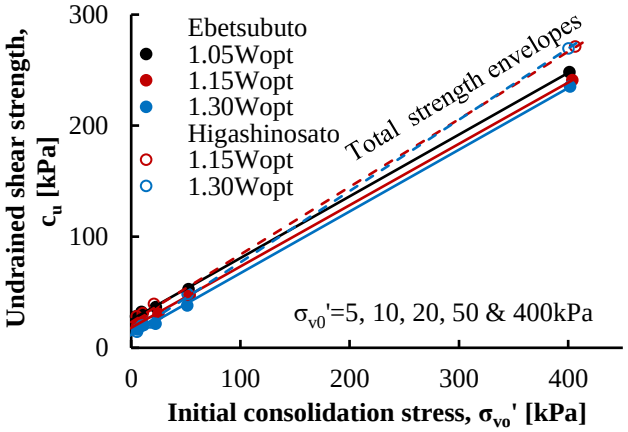

Fig. 5. Total stress strength envelopes for different states of Ebetsubuto and Higashinosato soils
soil

Table 2. Mohr–Coulomb (M-C) effective stress strength parameters for different states of Ebetsubuto and Higashinosato soils

Name of soils	States	M-C strength parameters		R^2
		Cohesion (c'), kPa	Friction (Φ'), °	
Ebetsubuto	$1.05w_{opt}$	11.2	32.8	0.99
	$1.15w_{opt}$	8.9	31.1	0.99
	$1.30w_{opt}$	3.9	32.5	1.00
Higashinosato	$1.15w_{opt}$	6.9	34.7	0.99
	$1.30w_{opt}$	3.1	35.6	0.99

Table 3. Mohr–Coulomb (M-C) total stress strength parameters for different states of Ebetsubuto and Higashinosato soils

Name of soils	States	M-C strength parameters		R^2
		Cohesion (c_{cu}), kPa	Friction (Φ_{cu}), ^{o}	
Ebetsubuto	$1.05w_{opt}$	25.3	29.0	0.99
	$1.15w_{opt}$	18.0	28.9	0.99
	$1.30w_{opt}$	11.6	29.0	0.99
Higashinosato	$1.15w_{opt}$	23.1	31.3	0.99
	$1.30w_{opt}$	12.8	32.7	0.99

B. Compression Characteristics

Fig. 6 shows the compression curves obtained from the Constant-Rate-of-Strain (CRS) tests on different states of Ebetsubuto soil. Additional tests were also performed by preparing samples with water content at an increment of $0.05w_{opt}$. The void ratios were calculated based on the initial dry density and finally checked with final water content after the test. The soil showed the compression curves of slightly flat gradients at low effective stresses, similar to over-consolidated soils. They tend to converge towards higher stress ranges, but without a distinct yield point. As all the curves are not completely parallel, but show a gentle convergence within the maximum applicable vertical stress of 3000kPa, it was therefore difficult to define a unique normal compression line unlike pure clays. Such non-parallel and non-convergence of compression curves along a unique normal compression line could be due to the presence of sand particles and their crushing during loading, and which produced the behavior similar to transitional soils and led to difficulty in defining a unique normal compression line [12]. To check the possibility of convergence along a unique normal compression line, if the compression takes place up to higher stresses, further work is needed.

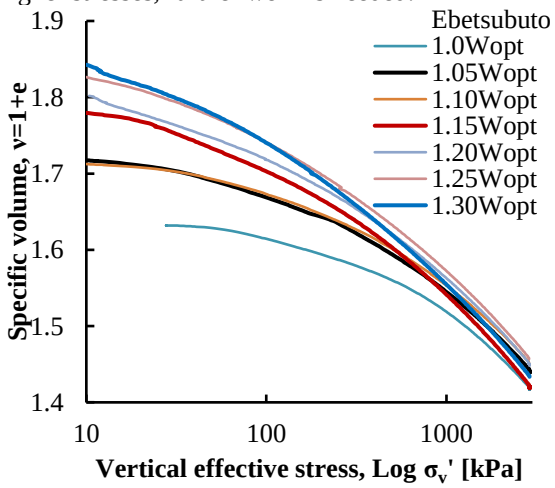

Fig. 6. Oedometer compression curves for different states of Ebesubuto soil

C. Compressive Strength and Deformation Characteristics

Fig. 7 shows the axial stress-strain curves for different states of Ebetsubuto and Higashinosato soils obtained from the unconfined compression tests. It can be seen from the figure that the axial stress-strain response is very stiff for the state at and closer to the optimum than that away from the optimum. At the optimum, the soil showed very brittle failure behavior with a distinct peak state (σ_a=400kPa at ε_a=3.84%) and dropped sharply without reaching residual strength. Moving towards the wetter sides, with increasing water content by $0.05w_{opt}$, the soil started showing softer responses with ductile failures by dropping peak stresses exponentially following the exponential equation, $\sigma_a=482.2e^{-0.07\varepsilon a}$. At the state of $1.30w_{opt}$, the soil exhibited most ductile behavior without a distinct peak state. The ductile behavior at the wetter side can be explained by the presence of single family of micro pores with continuous water phase and occluded air bubbles, which facilitates the individual particles sliding past each other, the lubrication effect increased with increasing water content, creating strain before failure. The resulting microstructure of clay is dispersed on the wetter side (single particle or particle group acting individually) [5-6].

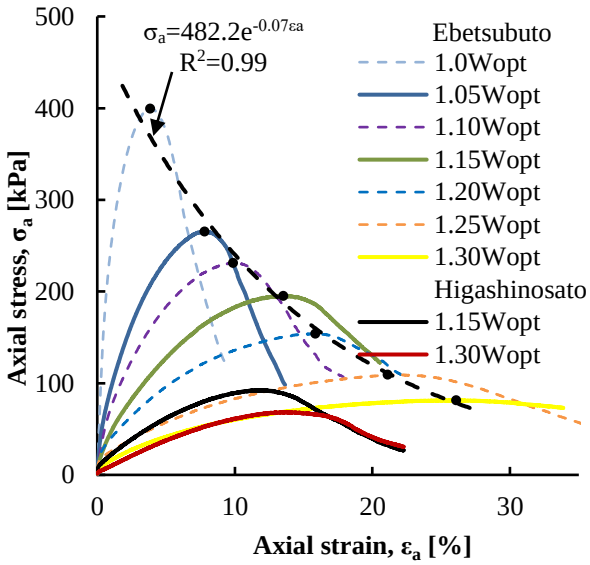

Fig. 7. Axial stress-strain curves for Ebetsubuto and Higashinosato soils from unconfined compression tests

Fig. 8 shows graphs of unconfined compressive strength against water content, dry unit weight and degree of compaction (measured after compaction). The unconfined compressive strength decreased with increasing water content, and increased with both increasing dry unit weight and degree of compaction. For Ebetsubuto soil, the unconfined compressive strength decreased from 400kPa to 81.3kPa with increasing water content from 22.6% to 31.7% and fitted well with a power function. The unconfined compressive strength

increased by the same amount when the dry unit weight increased from 13.9 to 15.4kN/m^3 and the degree of compaction increased from 88.9% to 98.4%, and fitted well with power functions. Consistent results can also be seen for Higashinosato soil, although only two data points are available. Using these curves, it is possible to estimate desired unconfined compressive strength by measuring moisture content or dry density or degree of compaction in the field.

Fig. 9 shows graphs of deformation modulus (E_{50}) against water content, dry unit weight and degree of compaction (measured after compaction). The deformation modulus is defined as a secant modulus which is calculated as the slope of a line from the origin through the point on the stress-strain curve at which the stress is one half of the unconfined compressive strength. The deformation modulus of soil was significantly high at the optimum and decreased gradually with increasing water content, and fitted well with a power function. The modulus decreased from 30.2MPa to 0.9MPa with increasing water content from 22.6% to 31.7%. Whereas the opposite was true when the dry unit weight increased from 13.9kN/m^3 to 15.4kN/m^3 and the degree of compaction increased from 88.9% to 98.4%. It should be noted that the deformation modulus was significantly high at the optimum water content (30.2MPa) in comparison to the consecutive state of 1.05w_{opt} (7.5MPa), which could be probably due to the effect of significantly high dry unit weight and suction creating high initial stiffness.

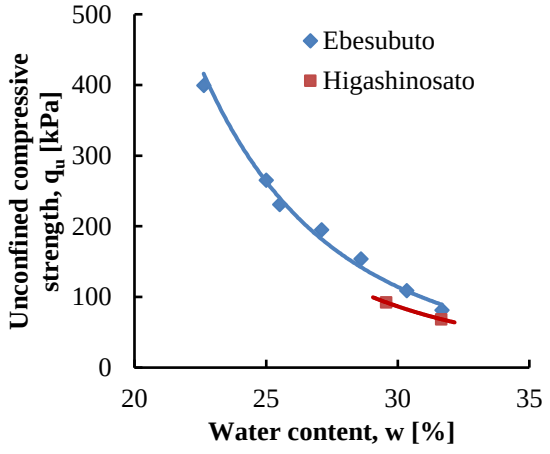

(a)

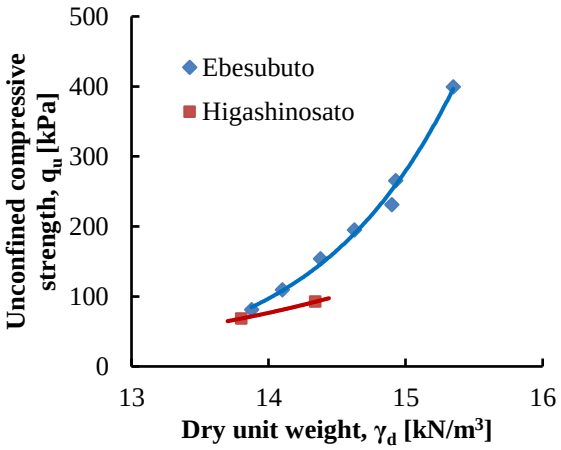

(b)

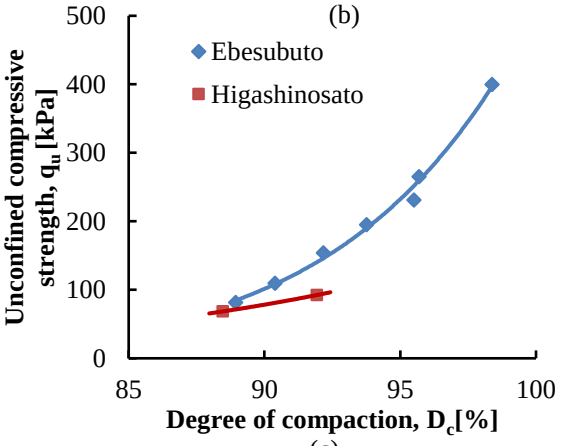

(c)

Fig. 8. Variations of unconfined compressive strength with (a) water content, (b) dry unit weight (c) degree of compaction

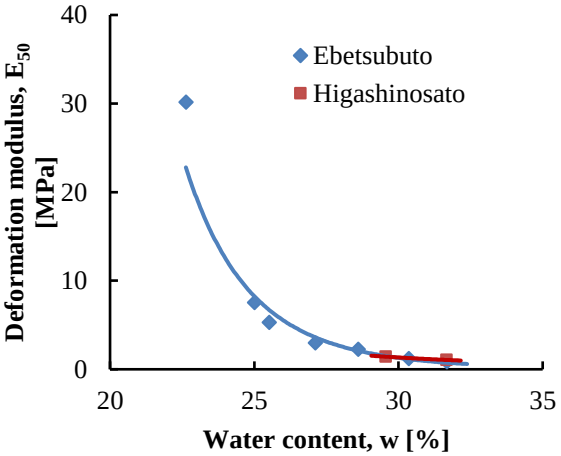

(a)

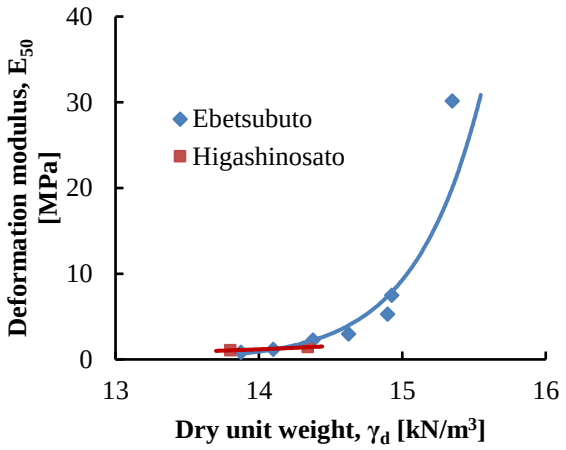

(b)

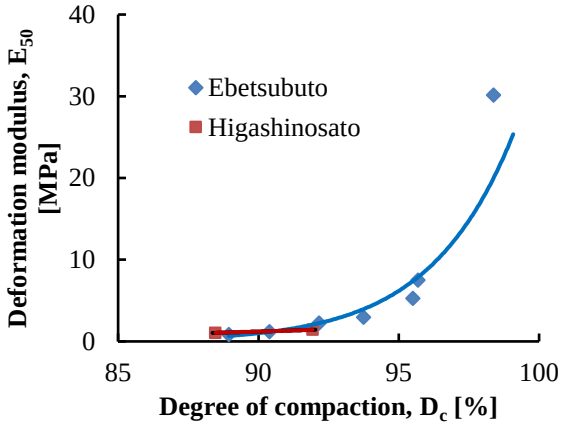

(c)

Fig. 9. Variations of deformation modulus (E_{50}) with (a) water content (b) dry unit weight (c) degree of compaction

V. CONCLUSIONS

Undrained strength behavior of compacted clay-sand mixed soils sampled from the river dyke construction sites were investigated by performing a series of constant-volume direct shear tests and unconfined compression tests. The compacted samples were prepared by adopting different states (defined with water contents and dry densities) on the wet side of optimum in standard proctor compaction tests. The undrained effective stress paths and strength envelopes for different states from the constant volume direct shear tests were analyzed, and the undrained strength parameters were derived. In addition, compressive strength and deformation modulus (E_{50}) from the unconfined compression tests were also determined. The following conclusions are drawn:

1. The undrained effective stress paths for each state exhibited initially modest contractive behaviour followed by strongly dilative behaviour with a distinct peak state at a low consolidation stress range (σ_{v0}'= 5-50kPa), whereas at a high consolidation stress range (σ_{v0}'= 400kPa) the stress paths exhibited contractive behaviour until reaching a failure state and then it moved along the failure envelope, showing the influence of coarser soil particles.The degree of dilation was more pronounced for the state closer to the optimum, which is controlled by the dry density or molding water content.
2. The effective strength envelopes for each state fitted well with the linear-Mohr Coulomb strength criterion but produced significant apparent cohesion for the state closer to the optimum as a result of high degree of dilation. It decreased gradually away from the optimum on the wetter side, whereas the angle of internal friction showed only smaller variations. The cohesion values are more sensitive to molding characteristics than the friction.
3. The compression curves for different states were not completely parallel, but showed gentle convergence within the maximum vertical stress of 3000kPa, which led to difficulty in defining a completely unique normal compression line similar to transitional soils unlike pure clays, probably due to the presence of coarser sand particles and their crushing during loading.
4. The axial stress-strain curves from unconfined compression tests exhibited very brittle failure behavior at a low strain for the state at and close to the optimum. The failure pattern changed gradually to ductile failure while moving away from the optimum. This can be explained by the single family of pores with continuous water phase in the compacted specimens on the wetter side of optimum, and higher water content lubricated the soil particles which facilitated the particles sliding past each other producing strain.
5. The unconfined compressive strength and deformation modulus increased with decreasing water content, and increasing dry unit weight and degree of compaction (measured after compaction) following power functions. Both were significantly high at the optimum water content in comparison to the consecutive other states on the wetter side, probably due to the effect of significantly high dry density and suction creating high initial stiffness in the stress-strain curves.

NOTATIONS

σ': Vertical effective stress
c', φ': Mohr-Coulomb effective strength parameters
w_{opt}: Optimum water content
w: Water content
w_L: Liquid limit
w_n: Natural water content
w_{opt}: Optimum water content
w_p: Plastic limit
G_s: Specific gravity
γ_d: Dry unit weight
σ'_{v0}: Initial vertical consolidation pressure
c_u: Undrained shear strength

φ_{cu}: Consolidated undrained angle of internal friction
c_{cu}: Consolidated undrained cohesion intercept
ε_a: Axial strain
σ_a: Axial stress
q_u: Unconfined compressive strength
E_{50}: Deformation modulus
R: Correlation coefficient

REFERENCES

[1] Alonso, E. E., Pinyol, N. M., & Gens, A. (2013). Compacted soil behaviour: initial state, structure and constitutive modelling. Geotechnique 63, No. 6, 463-478.
[2] Leonards, G. A. (1955). Strength characteristics of compacted clays. Trans. ASCE 120, 1420-1454.
[3] Seed, H. B. & Chan, C. K. (1959). Structure and strength characteristics of compacted clays. Journal of Soil Mechanics and Foundation Division, ASCE 85, No. SM5, 87-128.
[4] Kodikara, J., Islam, T., & Sounthararajah, A. (2018). Review of soil compaction: history and recent developments, Transportation Geotechnics 17 (Part B), 24-34.
[5] Lambe, T. W. (1958). The engineering behaviour of compacted clay. Journal of Soil Mechanics and Foundation Division, ASCE 84, No. SM2, 1-35.
[6] Lambe, T. W. & Whitman, R. V. (1969). Soil mechanics. New York, NY, USA, Wiley.
[7] Barden, L., & Sides, G. R. (1971). Engineering behaviour and structure of compacted clay, Journal of Soil Mechanics and Foundations Division, ASCE 96, No. 4, 1171-1197.
[8] Santucci De Magistris, F. & Tatsuoka, F. (2004). Effect of moulding water content on the stress-strain behaviour of compacted silty sand. Soils and Foundations 44, No. 2, 85-101.
[9] Heng, S., Pipatpongsa, T, Takemoto, M. & Yokota, S. (2010). Constant-volume direct box-shear test on clay seam materials, 17th Southeast Asian Geotechnical Conference, Taipei, Taiwan, May 10-13, 2010.
[10] Panta, A. (2018). Strength characteristics of fine-grained soils at dyke slope surfaces, PhD Thesis, Graduate School of Engineering, Hokkaido University.
[11] Panta, A., & Nishimura, S. (2017). Characterisation of state bounding surface at low effective stresses in clayey soils having different structures. Géotechnique 67, No. 6, 394-409.
[12] Coop, M. (2015). Limitations of a critical state framework applied to the behaviour of natural and transitional soils. Proceeding of. 6th International. Symposium of Deformation Characteristics of Geomaterials, Buenos Aires 6, 115-155.